Angiogenesis (2015) 18:361–371
DOI 10.1007/s10456-015-9472-7

ORIGINAL PAPER

Genome-wide expression analysis of wounded skin reveals novel genes involved in angiogenesis

Simone Brönneke[1] · Bodo Brückner[2] · Jörn Söhle[1] · Ralf Siegner[1] · Christoph Smuda[1] · Franz Stäb[1] · Horst Wenck[1] · Ludger Kolbe[1] · Elke Grönniger[1] · Marc Winnefeld[1]

Received: 8 December 2014 / Accepted: 20 May 2015 / Published online: 28 May 2015

Abstract Wound healing is a multistage process involving collaborative efforts of different cell types and distinct cellular functions. Among others, the high metabolic activity at the wound site requires the formation and sprouting of new blood vessels (angiogenesis) to ensure an adequate supply of oxygen and nutrients for a successful healing process. Thus, a cutaneous wound healing model was established to identify new factors that are involved in vascular formation and remodeling in human skin after embryonic development. By analyzing global gene expression of skin biopsies obtained from wounded and unwounded skin, we identified a small set of genes that were highly significant differentially regulated in the course of wound healing. To initially investigate whether these genes might be involved in angiogenesis, we performed siRNA experiments and analyzed the knockdown phenotypes using a scratch wound assay which mimics cell migration and proliferation in vitro. The results revealed that a subset of these genes influence cell migration and proliferation in primary human endothelial cells (EC). Furthermore, histological analyses of skin biopsies showed that two of these genes, ALBIM2 and TMEM121, are colocalized with CD31, a well known EC marker. Taken together, we identified new genes involved in endothelial cell biology, which might be relevant to develop therapeutics not only for impaired wound healing but also for chronic inflammatory disorders and/or cardiovascular diseases.

Keywords Angiogenesis · Genome-wide expression analyses · Human skin · Wound healing

Introduction

The term angiogenesis describes the growth of new blood vessels from preexisting ones. After a pro-angiogenic stimulus, endothelial cells (ECs), which form the inner lining of a vessel, start to break cell–cell contacts and secret proteases to degrade the basal membrane [1–3]. This degradation causes a feedback loop and intensifies the angiogenic process. In parallel, the expression of VEGF-A increases the permeability of ECs. Plasma proteins are secreted and build up a temporary matrix for the migrating ECs. Vessel sprouting is a hierarchical organized and coordinated process. It starts with the activation of a few endothelial cells—named tip cells—and is regulated by the Delta-like 4 (DII4)-Notch pathway [4–6]. The sprouting terminates when a tip cell has been attached to a close by (neighboring) vessel. In the following, EC secret factors such as platelet-derived growth factor B (PDGF-B) recruit mural cells (pericytes and/or smooth muscle cells) to the vascular wall [2, 7–9].

Although several factors involved in the angiogenic cascade have been already identified, only few genome-wide expression analyses have been conducted using human samples, yet. In order to investigate angiogenesis in human adults, we induced a wound healing process in skin by removing the epidermal layer. Wound healing is a

Elke Grönniger and Marc Winnefeld have contributed equally.

Electronic supplementary material The online version of this article (doi:10.1007/s10456-015-9472-7) contains supplementary material, which is available to authorized users.

✉ Marc Winnefeld
Marc.Winnefeld@Beiersdorf.com

[1] Research and Development, Beiersdorf AG, Hamburg, Germany

[2] Heidelberg, Germany

highly dynamic and complex process consisting of three partly overlapping steps: (i) inflammation phase, (ii) regeneration/tissue formation phase, and (iii) remodeling phase. All steps have to be aligned in a precise manner to restore tissue integrity [10–12]. The increased metabolic demands associated with wound healing require the formation and sprouting of new blood vessels to supply the surrounded tissue with oxygen and nutrients [11, 13–15].

In order to identify new angiogenic factors and to investigate how these factors are orchestrated during wound healing, skin samples from wounded and unwounded skin were obtained and genome-wide gene expression patterns were analyzed. A small set of genes that were differentially expressed during wound healing was identified. To characterize these genes regarding the angiogenic process in more detail, siRNA experiments using the scratch wound assay were performed. Thereby, we identified genes with a reduced proliferation and/or migration capacity after knockdown, suggesting that these genes—which have not yet been associated with angiogenesis—might be involved in dermal vasculature regeneration.

Materials and methods

Ethics statement

The recommendations of the current version of the Declaration of Helsinki as well as the international guidelines (e.g., FDA Regulations, GEP and AWB guidelines) were observed. Suction blistering was approved by the Freiburger Independent Ethics Committee (011/1973). Punch biopsies were obtained through a clinical study approved by the Hamburger Independent Ethics Committee (PV3424). Written informed patient consents were given from all volunteers.

Wounding of the skin by suction blistering and taking off the epidermal skin layer

In order to wound the skin, the epidermis was removed by suction blistering as described previously [16].

Tissue samples

Full-thickness skin samples (6 mm in diameter) were obtained from 14 volunteers by Sciderm GmbH (Hamburg, Germany). Punch biopsies of each volunteer were taken from wounded (suction blistering and removal of epidermis, sb) and unwounded skin (co) at four different time points (2, 4, 6, and 16 weeks after wounding). The wounded skin did not display any swelling or infection. All biopsies were isolated from the upper buttock to minimize depot specific variations.

In vivo capillary microscopy

In order to measure the density and morphologic patterns of capillary loops in the dermis, noninvasive capillary microscopy was performed using a CAM1V Video capillary microscope (Lawrenz Medizinelektronik). In total, eight female volunteers aged 66–72 years participated in the study. Before the investigations began, the patients were acclimated in a room with a constant temperature of 21 °C and 40 % humidity for 10 min. A drop of paraffin oil was applied to the skin to minimize reflection. To increase visibility of capillaries, venous stasis of 120 mm Hg on the forearm was done to maximize capillary blood load. Pictures were taken with the VRmagic CamLab Programm. Per volunteer and area, 7–9 pictures (0.65 mm^2) with 240-fold magnification were captured. Analyses of the pictures were performed with manual counting plus algorithmic calculation of the red area in percentage via the software ImageJ.

RNA isolation of skin biopsies

RNA from punch biopsy samples was processed with the NucleoSpin RNA II (Macherey–Nagel, Dueren, Germany) at the company ImaGene GmbH, Berlin. The biopsies, stored in liquid N_2, were put in −80 °C cooled tubes with glass beads and 4 µL 1 M dithiothreitol (DTT). After addition of 180 µL of lysis buffer (RA1), the tubes were restored in liquid nitrogen. To each sample, 170 µL RA1 buffer was pipetted and vortexed at 4 °C for 15 min to gain homogenization. Following, RNA was isolated as recommended by the supplier.

Quantitative RT-PCR

The TaqMan Gene Expression Assay (Applied Biosystems, Foster City, USA) was used to analyze the knockdown efficiency of the siRNA-transfected endothelial cells. RNA was reverse-transcribed into cDNA, and PCRs were carried out in triplicate as recommended by the manufacturer. Quantitative RT-PCR of the genes ABLIM2 (Assay ID Hs00287164_m1), FGFR-1 (Assay ID Hs00915142_m1), GGCT (Assay ID Hs01031800_g1), SULF2 (Assay ID Hs01016476_m1), TMEM (Assay ID Hs00846437_s1), and ZSCAN18 (Assay ID Hs00225073_m1) (all Applied Biosystems, Foster City, USA) were performed using the Applied Biosystems 7900HT Fast Real Time PCR System. C_T values were calculated by the RQ Manager software 1.2. Target gene expression was normalized on expression of the endogenous control GAPDH (Assay ID Hs99999905_m1), and calculations were performed using the comparative C_T method [17].

Cultivation of human dermal endothelial cells

Primary microvascular endothelial cells isolated from female skin were obtained from Lonza (Walkersville, USA). Cell populations of three donors aged between 32 and 50 were pooled (Lot 0000122821, 0000125583, and 0000125028) and used in passage 4. Endothelial cells were cultured as previously described [18].

SiRNA transfections of endothelial cells using Lipofectamine

SiRNAs (Qiagen, Hilden, Germany) and lipofectamine (Lipofectamine 2000, Invitrogen) were mixed according to the manufacturer's instructions but only with half of the denoted lipofectamine volume. Multiwell pipetting was performed using Biomek FXp Laboratory Automation Workstation (Beckman Coulter, USA). The mix was loaded into 96-well plates with a final concentration of 50 nM siRNA. Manually, a total of 7500 cells were plated directly into the transfection mix. The next day, cells were washed and medium was changed to Endothelial Cell Basal Medium-2 (EBM-2) (Lonza, Walkersville, USA) containing 5 % fetal bovine serum (FBS) and gentamycine (GA) (both Lonza, Walkersville, USA). After 24 h of incubation, scratch wound assay was performed.

Three different siRNAs per target were investigated, while siFGFR-1 (SI03066098) served as a positive control and the scrambled siRNA (SI03650325) as a negative control (both obtained from Qiagen, Hilden, Germany) on every 96-well plate. The entire library of 144 siRNAs (for sequences, see supplemental table S2) was screened twice.

Scratch wound assay

After 48 h post-transfection, a scratch was created in the confluent cell monolayer using pipette tips (Biomek AP96 P250, Beckman Coulter, USA) driven by Biomek FXp Laboratory Automation Workstation (Beckman Coulter, USA). Afterwards, plates were washed once with PBS and refilled with EBM-2 medium supplemented with 10 ng/mL of recombinant fibroblast growth factor 2 (FGF-2) (Gibco, Karsruhe, Germany). Migration and proliferation of transfected cells were measured at a fixed time point 30 h after scratching. The monolayer of dermal microvascular endothelial cells was washed with phosphate-buffered saline (PBS, Lonza, Walkersville, USA) and fixed with 2 % formaldehyde solution (36.5–38 % formaldehyde solution from Sigma–Aldrich, Taufkirchen, Germany) for 15 min. The cells were stained with propidium iodide (5.5 μg/mL, Invitrogen, Karlsruhe, Germany) and analyzed using a fluorescence microscope Axiovert S100 (Carl Zeiss Mikroskopie, Goettingen, Germany). Migration/proliferation rates were monitored by measuring the reduction of cell-free area by thresholding for dark objects at Wimasis Image Analysis GmbH (Munich, Germany). The rate of migration and proliferation was measured by quantifying the total area that the cells moved from the edge of the scratch toward the center of the scratch. Directly after wounding, the scratch area was determined in 36 repeats and regarded as a constant with 5.72 mm^2.

Cell viability assay

After siRNA transfection, cell viability was measured using Cell-Titer-Blue-Cell Viability Assay (Promega, Fitchburg, USA). The protocol was performed according to the manufacturer's instructions. The reagent was added 48 h after transfection to the cells, and viability was monitored. Cells treated for 24 h with cytotoxic cis-diammineplatinum(II)dichloride (10 μg/mL) (Sigma-Aldrich, Taufkirchen, Germany) served as a negative control.

Caspase-Glo 3/7 assay

After siRNA transfection, apoptotic activity was measured using the Caspase-Glo 3/7 Assay (Promega, Fitchburg, USA). The protocol was performed as recommended by the supplier. Transfected cells were analyzed 48 h after knockdown. Cells treated for 24 h with staurosporine served as negative control.

Array-based gene expression analysis

In order to identify differentially expressed genes in wounded and unwounded skin, samples were analyzed using one-color Whole Human Genome Microarray 4 × 44 K chips from Agilent Technologies which were carried out by ImaGene GmbH (Berlin, Germany).

Immunohistochemistry staining (IHC) of human skin biopsies

To analyze CD31 protein expression in skin tissues, samples were paraffin-embedded, sectioned at 2–5 μm, and mounted on glass slides. Sections were deparaffinized by heating slides to 100 °C and incubating in DAKO Target Retrieval Solution (Glostrup, Dänemark, pH 6.1, diluted 1:10) for 20 min. Afterwards, slides were carefully washed with demineralized water. All immunohistochemical steps were performed using EnVision Gl2 doublestain system as recommended from the supplier (DAKO, Glostrup, Denmark). Monoclonal CD31 antibodies (DAKO, Glostrup, Denmark) were diluted 1:30 in DAKO antibody-diluting agent and incubated on slides for 30 min. The hematoxylin staining was performed according to DAKÓs instruction.

After staining, sections were air-dried at RT. In the following, sections were sealed with Leica CV Ultra mounting medium (Nussloch, Germany) and glass coverslips.

Immunofluorescence microscopy of human skin biopsies

To verify expression of identified genes on protein level in wounded skin, appropriate paraffin-embedded tissue Sections. (2–5 µm, mounted on glass slides) of punch biopsies obtained from wounded skin (suction blister) were stained by immunofluorescence technique. TMEM121 and ABLIM2 primary antibodies were purchased from ABCAM (ab151077, ab100926, Cambridge, Great Britain). Endothelial cells were stained using CD31 antibody from DAKO (M0823 Glostrup, Denmark). AF488 and AF594 from Life Technologies GmbH (Darmstadt, Germany) were used as secondary antibodies. Sections were deparaffinized by a 100 °C incubation in DAKO Target Retrieval Solution (Glostrup, Denmark, pH 6.1) for 20 min. Afterwards, slides were carefully washed with demineralized water and stained as follows: blocking with antibody dilution buffer (DCS Innovative Diagnosik-Systeme, Hamburg, Germany) for 90 min, treating with primary antibody for 60 min, washing two times with antibody dilution buffer for 5 min each, incubating with secondary antibody for 60 min, washing once as described above, and finally staining the nuclei with Hoechst 33342 (Life Technologies GmbH, Darmstadt, Germany). Between all steps, slides were rinsed thoroughly with DPBS (Sigma-Aldrich, Steinheim, Germany).

Data deposition

The microarray data set is available in the Gene Expression Omnibus database http://www.ncbi.nlm.nih.gov/geo/query/acc.cgi?token=ctipmieixtsrhcd&acc=GSE56803, under the accession number GSE56803.

Statistical analyses

The preprocessing and quality control of microarray data were performed as previously described [18]. To identify genes differentially expressed in wounded versus unwounded skin, the limma package for the R statistical software was used. Few samples were excluded because they showed "outlier" characteristics. Supplement Table 1 summarizes the information about the cleaned set of samples.

For the quantitative RT-PCR analyses of the genes ABLIM2, FGFR-1, GGCT, SULF2, TMEM121, and ZSCAN18, as well as for the FGF-2-induced cell migration, and for the scratch wound analyses, Statistica 9.1 (StatSoft, Hamburg, Germany) and GraphPad Software Prism 5 (La Jolla, USA) were used. Normal distribution was checked by means of Shapiro–Wilk's test, and unpaired *t* test was performed. A significance level of 0.05 (alpha) was chosen for statistical analyses, based on two-sided hypothesis testing.

For analyses of vascular changes after suction blistering and removal of the epidermis, GraphPad Software Prism 5 (La Jolla, USA) was used and repeated-measures ANOVA was performed. A significance level of 0.05 (alpha) was chosen for statistical analyses. Functional categories and pathway analyses of differentially expressed genes were generated by the use of IPA (Ingenuity® Systems, www.ingenuity.com).

Results

Capillary density is increased after human epidermal wounding

To establish an appropriate in vivo model to analyze angiogenic processes in the human skin, a pilot study was conducted. Therefore, we wounded human skin by removing suction blister roofs from the upper arm of eight human volunteers [19, 20]. Besides ethical reasons, the advantage of wounding only the upper skin layer is that even to an early time point (after 2 weeks) skin was completely healed and the epidermis was regenerated (Fig. 1a). As the epidermal compartment lacks vessels and is supplied with oxygen and nutrients by the papillary dermal vasculature [21–23], we first investigated whether the wounding of the epidermis is sufficient to stimulate dermal vessel growth and remodeling. Therefore, vessel density was examined before wounding, and 2, 4, 6, and 16 weeks after wounding using capillary microscopy (Fig. 1b). Unwounded skin of volunteers aged between 66 and 72 years (control areas) was characterized by unstructured morphological arrangements and an average capillary density of 13 capillaries per mm^2 (Fig. 1c). In contrast, 2, 4, and 6 weeks after wounding, the microvessel density in the dermis increased significantly compared to control areas. In addition, a more structured and organized morphology and distribution was observed. The maximum increase in microvessel density (28 capillaries/mm^2) was determined 2 weeks after wounding. After 16 weeks, the number of capillaries decreased comparable to control levels. To verify the results with an independent analysis method, we determined the percentage of total visible vessels using the same sample set. After 2, 4, and 6 weeks post-wounding, the "visible vessel area" increased significantly from 6.8 to 17.0 % per mm^2 (Fig. 1d). Again, after 16 weeks post-wounding, the visible vessel area was

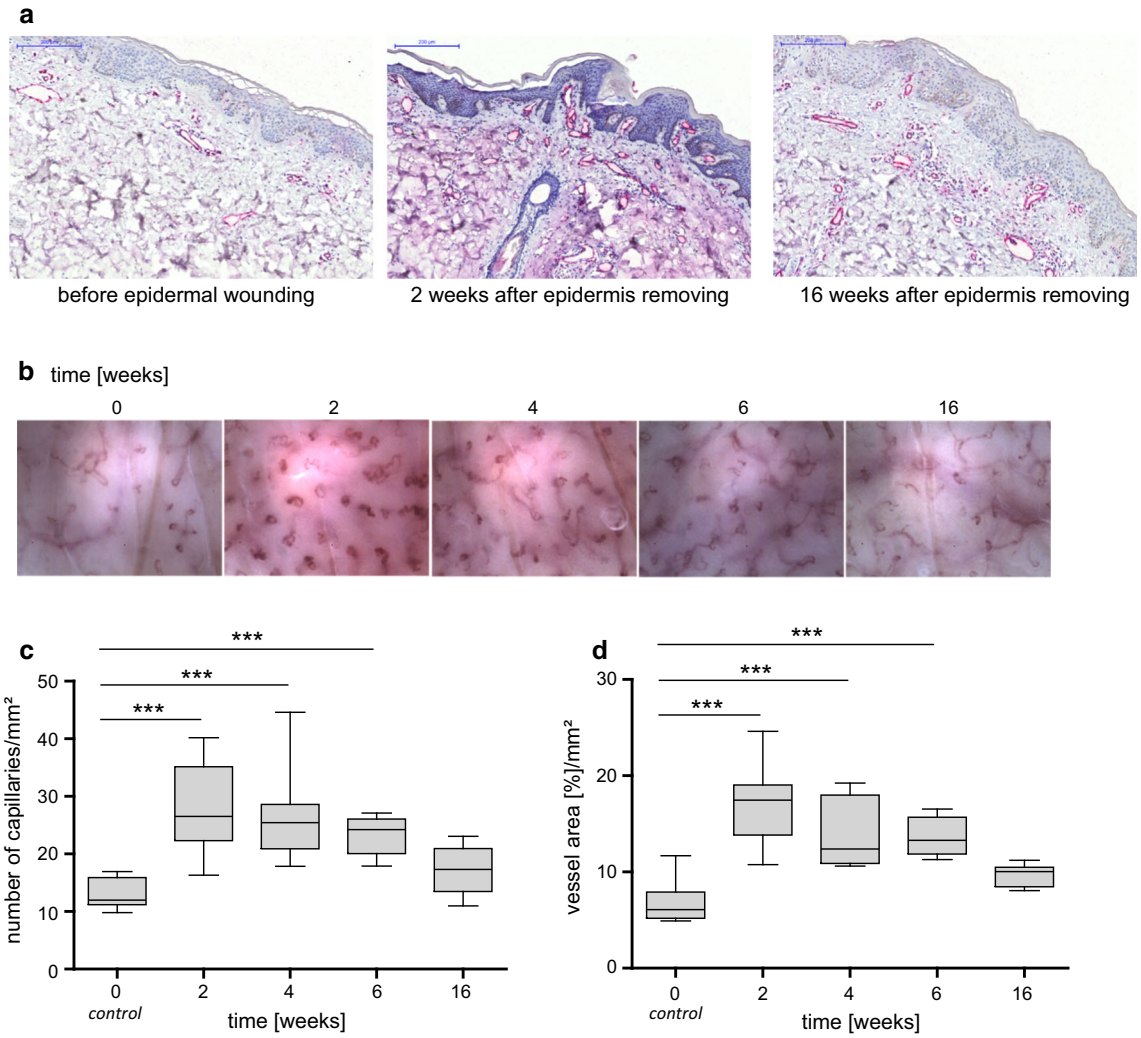

Fig. 1 Vascular changes after epidermal wounding. **a** Images of IHC staining (CD31) of biopsies obtained before wounding, 2 and 16 weeks after suction blistering. *Bar*: 200 µm. **b** Images captured by capillary microscopy are shown for one representative volunteer at five different time points. Per volunteer, 7–9 pictures were captured each, with an area of 0.65 mm^2. **c** Numbers of capillaries and **d** area of visible vessels per mm^2 were quantified to the according time points. The *horizontal black lines* denote medians and whiskers the 2.5th and 97.5th percentiles. Significant differences are indicated by asterisks. $*p \leq 0.05$; $**p \leq 0.01$; $***p \leq 0.001$ (repeated-measures ANOVA). $n = 8$

insignificantly elevated, indicating that vessel formation is induced and stable up to 6 weeks after suction blistering.

Taken together, removing the epidermis without wounding the dermis is sufficient to stimulate capillary reorganization and/or regeneration.

Identification of differentially expressed genes after epidermal wounding

In order to identify genes being involved in angiogenesis during human wound healing, we determined the mRNA transcription profile of unwounded and wounded skin using Agilent Whole Human Genome Microarrays, which allow the analysis of 45,015 gene probes. For the analyses, ten female and four male volunteers were wounded by suction blistering, and 2, 4, 6, and 16 weeks after wounding, punch biopsies were obtained from wounded (sb) and unwounded skin (co) of each volunteer (Fig. 2a). The time points have been chosen because the epidermis of wounded skin needed at least 2 weeks to recover completely. Therefore, an earlier time point—with an incomplete recovered epidermis—would have caused biased microarray results, simply because different tissue compositions would have been analyzed (Figs. 1a, 2b). Before starting the analyses of the transcription profiles, the microarray data were preprocessed and filtered to remove low-quality probes. Next, the processed data were subjected to a panel of sample quality metric functions (supplement Fig. S1). The

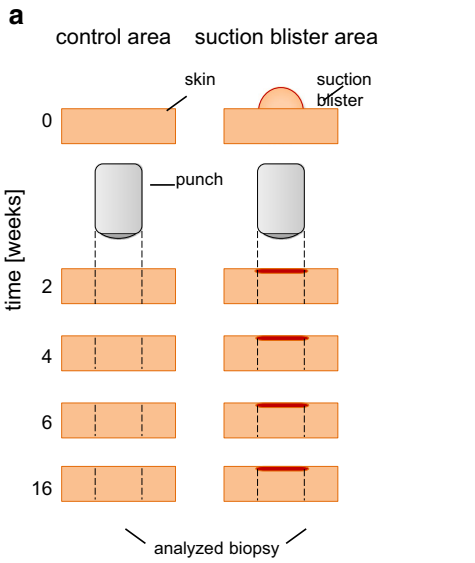
a
control area
suction blister area
skin
suction blister
0
punch
time [weeks]
2
4
6
16
analyzed biopsy

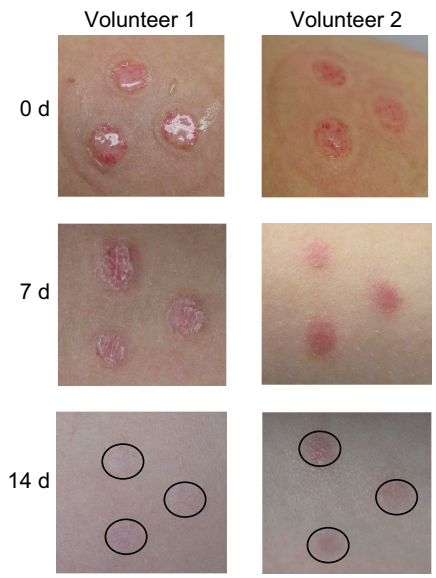
b
Volunteer 1
Volunteer 2
0 d
7 d
14 d

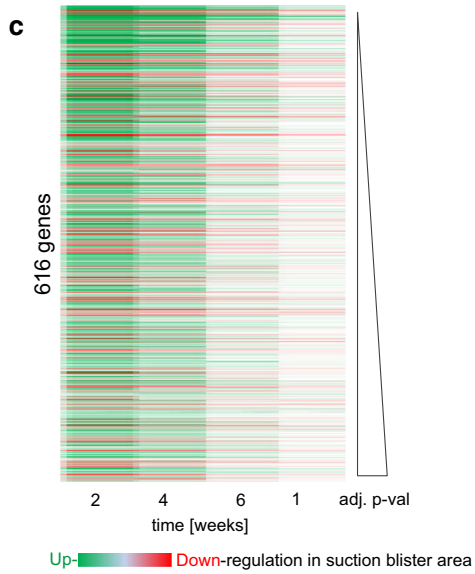
c
616 genes
2
4
6
1
adj. p-val
time [weeks]
Up-
Down-regulation in suction blister area

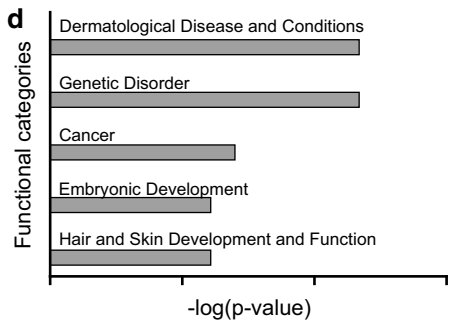
d
Functional categories
Dermatological Disease and Conditions
Genetic Disorder
Cancer
Embryonic Development
Hair and Skin Development and Function
-log(p-value)

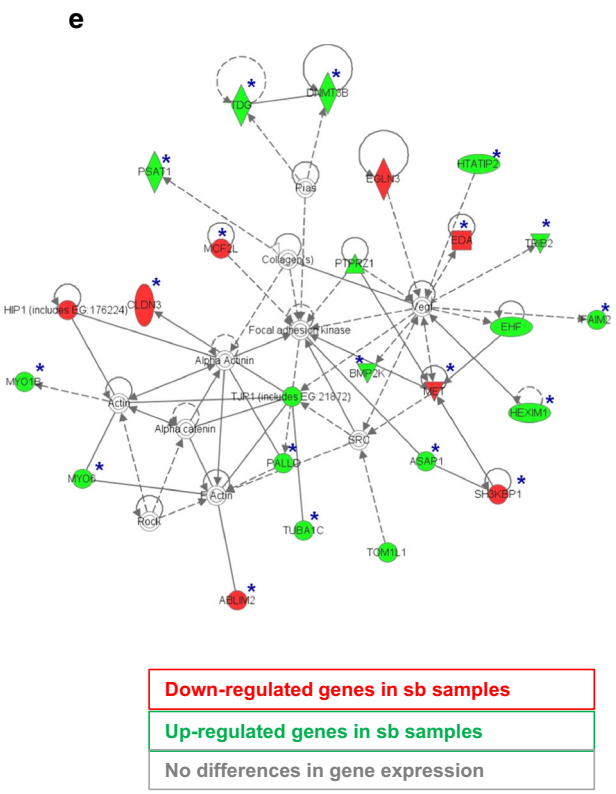
e
Down-regulated genes in sb samples
Up-regulated genes in sb samples
No differences in gene expression

◀**Fig. 2** Differentially expressed genes during human wound healing. **a** Schematic overview of the combined wounding (suction blistering) and punch biopsy study. Two, 4, 6, and 16 weeks after suction blistering, full-thickness skin samples were obtained and RNA was isolated for microarray analyses. **b** Images of wounded skin areas are shown for two representative volunteers (before wounding (d0), 7 and 14 days after suction blistering (d7 and d14). **c** The heat map shows the 616 differentially expressed genes between wounded (sb) and unwounded (co) skin samples at the four different time points. The *rows* are scaled according to increasing p values (BH adj. $p \leq 0.01$). **d** Top five functional categories for differentially regulated genes in wounded (sb) versus unwounded (co) skin samples derived from Ingenuity Pathway Analysis (IPA). **e** Top network built by up-regulated and down-regulated genes in sb samples obtained by IPA. Genes with a *blue asterisk* are expressed in human dermal microvascular endothelial cells

processed microarray data (table S1) comprised on each array 30,317 significant gene probes, which corresponded to 15,222 genes. In total, 810 transcript variants were significantly differentially expressed between co and sb samples during the time course of 16 weeks, as visualized by the heat map (Fig. 2c). The 810 transcript variants corresponded to 577 up-regulated and 233 down-regulated transcripts in sb compared to co samples (Benjamini Hochberg adj. p val <0.01). The strongest expression change was detected 2 weeks after wounding. After 4 and 6 weeks following wounding, expression change intensities decreased, resulting in a comparable level between co and sb samples after 16 weeks. The course of expression changes is therefore in good agreement with the changes in microvessel density which also decreased at later time points (Fig. 1c, d). The 810 transcript variants could be assigned to 616 genes. Only three gene probes were differentially expressed between male and female samples, indicating that gender-specific differences play only a minor role.

Supplement table S2 summarizes those genes out of the 616 differentially expressed genes between co and sb samples that are known to be involved in angiogenesis. To further analyze the biological relevance of the 616 differentially expressed genes, network and functional analyses were performed using IPA (Ingenuity Pathway Analysis, Ingenuity® Systems, www.ingenuity.com). Differentially expressed genes were enriched in functional categories such as "dermatological disease and conditions, genetic disorders, cancer, embryonic development," and "hair and skin development and function" (Fig. 2d). These functions were further specified by subcategories such as "development of epidermis, synthesis of melanin, differentiation of epidermal cells and melanocytes, and innervation of skin." The third top-score network named "cellular movement, tumor morphology, cell to cell signaling and interaction" (Fig. 2e). Interestingly, a variety of interacting proteins of the vascular endothelial growth factor (VEGF) family (f. e. VEGF-A, VEGF-B, VEGF-C, VEGF-D) were up-regulated or down-regulated during the 16-week progress of wound healing. VEGF proteins play important roles in angiogenesis [24–26], and although the members of this family were not directly affected in our model system, it can be speculated that the deregulation of interacting proteins could contribute to angiogenesis.

Overlap between differentially expressed genes during wound healing and gene expression in cultured endothelial cells

For our analysis, full-thickness skin samples have been used containing a variety of different cell types such as keratinocytes, fibroblasts, immune cells, and endothelial cells. To investigate whether the differentially expressed genes are also expressed in cultured human microvascular ECs, we compared the 616 differentially expressed genes during wound healing to 13,406 genes which are known to be expressed in cultured endothelial cells [18]. A total of 438 genes overlapped, as indicated by the Venn diagram (Fig. 3), suggesting that a great proportion (>70 %) of differentially expressed genes might be relevant for endothelial cell behavior. To further characterize this gene set, we selected those genes that showed in addition a twofold change in gene expression during wound healing. In total, 48 genes have been selected by these criteria (table S3 and S4).

Functional characterization of differentially expressed genes during wound healing using siRNA transfection in cultured endothelial cells

To further analyze the functional relevance of the 48 selected genes on angiogenesis, siRNA-induced knockdown experiments have been conducted in primary endothelial cells. To characterize the endothelial phenotypes after siRNA treatment, we performed scratch wound assays. This method considers two aspects of wound healing as

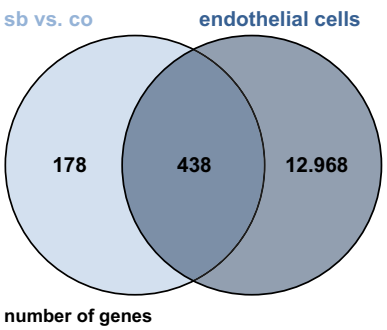

Fig. 3 Comparative gene expression analysis. The *Venn diagram* shows the overlap of genes with a differential expression pattern in wounded (sb) versus unwounded (co) samples as well as expression in human dermal endothelial cells

endothelial cells migrate and proliferate after activation by FGF-2 into a denuded area to close the wounded cell layer [27, 28].

As a positive control for impaired endothelial migration and proliferation, we targeted the receptor of FGF-2, FGFR-1 (FGF-2 receptor, fibroblast growth factor receptor 1) [28]. The siRNA-induced knockdown of FGFR-1 resulted in down-regulation of FGFR-1 mRNA up to 70 % (supplement Fig. S2 a). Compared to scrambled siRNA treatment (set as 100 %), knockdown of FGFR-1 significantly reduced endothelial cell proliferation and/or migration as the scratch area was only closed by 57 % (supplement Fig. S2 b). Viability was comparable between transfected and control-transfected cells, indicating that the reduced wound closure was not caused by an increased cell death (see supplement Fig. S2 c).

In the following, we used the scratch wound assay to analyze the knockdown phenotypes of the 48 genes. To reduce off target effects, 3 siRNAs per gene were investigated, and each of the 144 siRNA transfections was performed in sextuple. To be scored as a hit, at least 25 % decreased wound closure has to be observed after transfection with two different siRNAs. In total, five genes—ABLIM2 (actin-binding LIM protein family, member 2), ZSCAN18 (zinc finger and SCAN domain containing 18), GGCT (γ-glutamylcyclotransferase), SULF2 (Sulfatase 2), and TMEM121 (transmembrane protein 121)—have been identified, which showed a decreased migration and/or proliferation capacity in primary human endothelial cells (Fig. 4a–e). The significant reduction of mRNA levels after knockdown of these genes can be seen in supplement Fig. S3 a–e. In addition, we could exclude the possibility that the observed phenotypes have been caused by an increased cell death of the transfected cell populations. Neither cell viability nor apoptotic activity was significantly affected after knockdown of the corresponding gene (supplement Fig. S4 a and b).

To investigate whether altered proliferation or migration resulted in the observed phenotype, we determined the total cell number by propidium iodide staining (supplement Fig. S5). The siFGFR-1-transfected cells showed an average decrease of 26 % in cell number compared to scrambled siRNA-treated cell populations. However, the average decrease in wound closure was calculated to 57 %. The knockdown of the other genes impaired cell proliferation as well. For all genes, we observed that the phenotype "Reduced wound closure" was slightly more prominent than the proliferation defects (reduced cell number). The results of all genes are summarized in supplement Fig. S5. Therefore, we speculate that the identified genes affect not only EC proliferation but also EC migration although to a lower extent and could therefore contribute to two important processes during angiogenesis.

Histological analysis of AMBIM2 and TMEM121 during wound healing

To determine whether the identified genes are expressed during wound healing, histological analyses were performed using skin samples taken 2 weeks after wounding. For GGCT, SULF2, and ZSCAN18, a variety of different antibodies have been tested. Unfortunately, we could not detect a specific staining for those proteins. For ABLIM2 and TMEM121, a colocalization with CD31-positive structures (Fig. S6 A-D) was observed, suggesting that these two proteins might be involved in the regeneration of the dermal vasculature. For GGCT, SULF2, and ZSCAN18, additional analyses are needed to clarify their exact role during wound healing.

Discussion

To analyze angiogenic processes during cutaneous wound healing, we removed the epidermis without wounding the dermis to stimulate capillary reorganization. While we observed a recovery of the initial state already after 16 weeks, wounding of the epidermis and dermis led to an increase in capillary density even after 52 weeks post-surgery as Brown et al. described [29]. This difference can be explained by the depth of wounding and might correlate with stronger wound healing reactions. However, the advantage of wounding only the upper skin layer is that even to an early time point (after 2 weeks) skin was completely healed and skin biopsies of wounded and unwounded skin were homogenous in structure and thus comparable for genome-wide mRNA expression profiles.

So far, there are only a few dermatological studies available, analyzing genome-wide expression patterns of wounded and unwounded skin in humans. One study summarized results regarding angiogenesis in chronic human wounding. The authors used laser microdissection to isolate blood vessels from unwounded and wounded human skin [30]. The overlay between this analysis and our data set is minor which is most likely caused by the different study designs.

Several microarray experiments have been performed in mice to identify genes that are differentially expressed during wound healing [31, 32]. In one of these studies, Roy and coworkers investigated the acute temporal changes in excisional murine cutaneous wound inflammation by analyzing the wound-edge transcriptome [33]. Although rodents have dense hair, relatively thin epidermal and dermal layer, and wound healing happens mainly by contraction and not by re-epithelialization [34], an overlap of differentially expressed genes has been observed between both studies. Interestingly, five genes named CCL3, MX1,

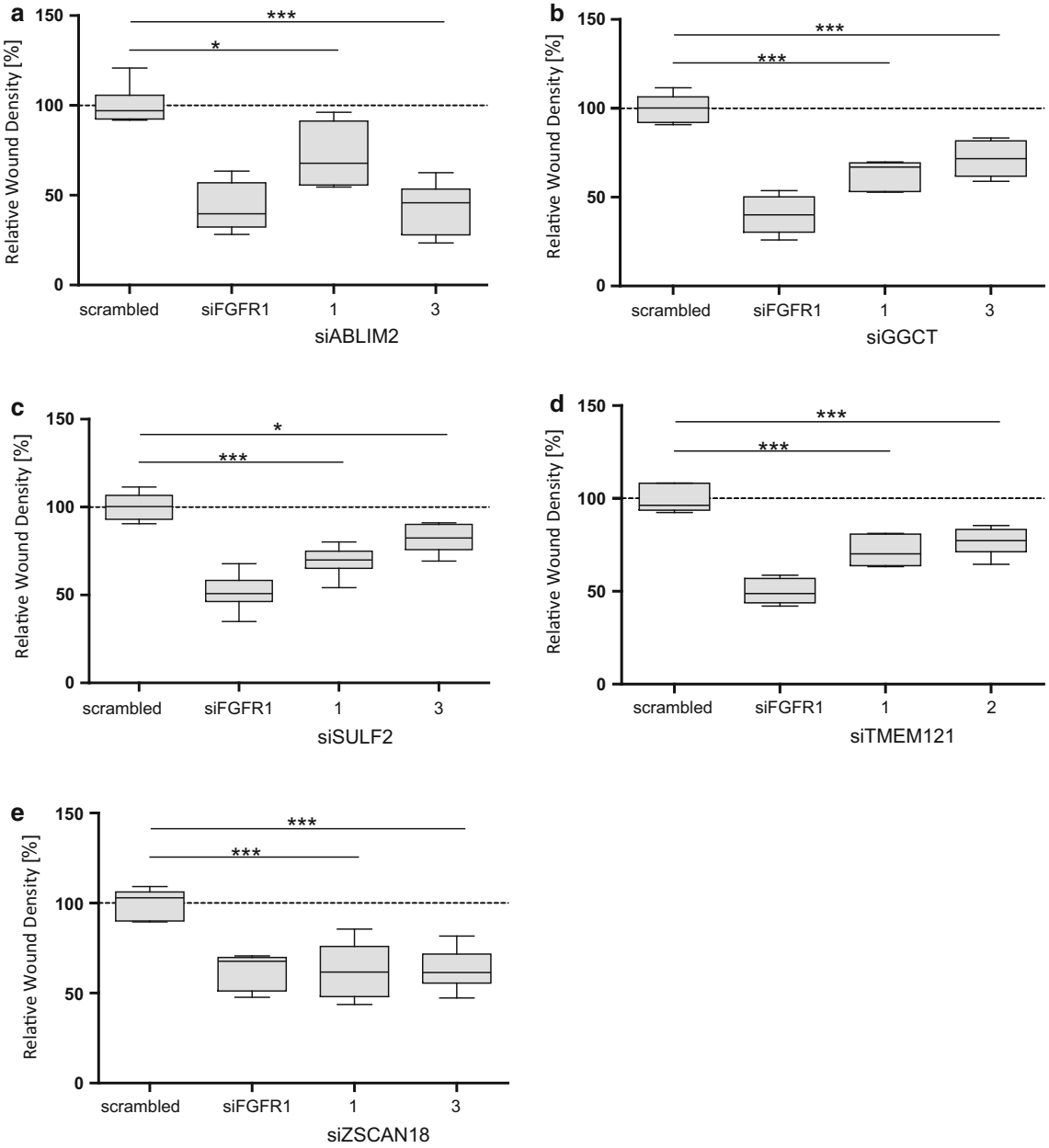

Fig. 4 Genes showing a pro-angiogenic phenotype in wound healing assay in vitro. Primary blood endothelial cells were transfected with three different siRNAs per gene, indicated by the number 1, 2, or 3 (only the two most potent ones are depicted). After 48 h post-transfection, a scratch was created in the confluent cell monolayer and the Relative Wound Density (RWD) was measured in % 30 h post-wounding. The RWD of scrambled siRNA-transfected cells was set as 100 %. The RWD is shown for the knockdown of genes **a** ABLIM2, **b** GGCT, **c** SULF2, **d** TMEM121, and **e** ZSCAN18 induced by the two most effective siRNAs. The average value of the scrambled control is shown as the *dotted line*. The *horizontal black lines* denote medians and whiskers the 2.5th and 97.5th percentiles. Significant differences are indicated by asterisks. $*p \leq 0.05$; $**p \leq 0.01$; $***p \leq 0.001$ (unpaired *t* test). *n* (per siRNA) = 6

ARG1, MARCKSL1, and PIK3CD are overexpressed in wounded skin of mice and humans. All genes are highly expressed in macrophages which are known to be important players in wound healing [35]. However, it should be noted that these similarities have only be observed on the mRNA expression levels. Therefore, the biological relevance for mice and humans has to be determined in more detail in future studies.

To investigate the molecular processes of human angiogenesis more precisely, we selected genes (1) showing at least a twofold change in gene expression during wound healing and (2) being expressed in primary human endothelial cells. To test the functional relevance, siRNA experiments have been performed. The knockdown phenotypes were analyzed using the well-established scratch wound assay [28]. We could identify five genes that—to

the best of our knowledge—have not yet been described to be involved in endothelial cell proliferation and/or migration. The expression patterns of these genes during the wound healing process are shown in detail in supplement table S5. In addition, histological analysis revealed that ABLIM2 and TMEM121 colocalize with CD31-positive structures (supplement Fig. S6). Although all genes are expressed in a variety of different cell types (supplement Fig. S7), most of them are rarely described in the scientific literature. For ZSCAN18 (zinc finger and SCAN domain containing 18) and GGCT (γ-glutamyl cyclotransferase), it is known that they are involved in proliferation and/or migration. However, these analyses have been performed in cancer or primary kidney cells [36]. TMEM121 (transmembrane protein 121) has been shown to be a repressor of MAP kinase signaling [37]. For ABLIM2 (actin-binding LIM protein family, member 2), it is speculated that this gene is important in the guidance of axons [38]. As endothelial sprouting and axonal growth share some similarities [39], ABLIM2 might also play a role in the guidance of tip and neighboring cells. SULF2 (sulfatase 2) was another interesting gene that has been identified in our study. Factors of the FGF family act with heparin and heparan sulfate proteoglycans to activate FGF receptors [40]. This interaction depends among others on sulfatases, which was f. e. studied in chondrocytes [41]. A contrary view was published by Peterson et al. [42], showing that SULF2 impairs tumor growth without any effect on vessel density. This contrary observation might be explained as cancerous blood vessels show divergent cellular abnormalities [43, 44]. Heterozygous SULF1$^{-/-}$ and SULF2$^{-/-}$ mice suffer from reduced neurite sprouting [45], and again a parallel between vessel and nerve guidance might be drawn.

Although future studies will be needed to clarify the exact role of these genes in stimulating angiogenesis during wound healing, the set of differentially regulated genes which additionally has impact on endothelial cell behavior in vitro may provide important insights into how human wound angiogenesis is orchestrated.

Acknowledgments We thank Sonja Wessel, Boris Kristof, and Thomas Lange for helpful discussions and support concerning capillary microscopy and analyses.

Conflict of interest All authors were employees at Beiersdorf at the time point of the study. B. Brückner received consultation fees from Beiersdorf.

References

1. Adams RH, Alitalo K (2007) Molecular regulation of angiogenesis and lymphangiogenesis. Nat Rev Mol Cell Biol 8(6):464–478
2. Herbert SP, Stainier DY (2011) Molecular control of endothelial cell behaviour during blood vessel morphogenesis. Nat Rev Mol Cell Biol 12(9):551–564
3. Carmeliet P, Jain RK (2011) Molecular mechanisms and clinical applications of angiogenesis. Nature 473(7347):298–307
4. Phng LK, Gerhardt H (2009) Angiogenesis: a team effort coordinated by notch. Dev Cell 16(2):196–208
5. Gerhardt H (2008) VEGF and endothelial guidance in angiogenic sprouting. Organogenesis 4(4):241–246
6. Jakobsson L et al (2010) Endothelial cells dynamically compete for the tip cell position during angiogenic sprouting. Nat Cell Biol 12(10):943–953
7. Inai T et al (2004) Inhibition of vascular endothelial growth factor (VEGF) signaling in cancer causes loss of endothelial fenestrations, regression of tumor vessels, and appearance of basement membrane ghosts. Am J Pathol 165(1):35–52
8. Bergers G, Song S (2005) The role of pericytes in blood-vessel formation and maintenance. Neuro Oncol 7(4):452–464
9. Armulik A, Abramsson A, Betsholtz C (2005) Endothelial/pericyte interactions. Circ Res 97(6):512–523
10. Gurtner GC et al (2008) Wound repair and regeneration. Nature 453(7193):314–321
11. Singer AJ, Clark RA (1999) Cutaneous wound healing. N Engl J Med 341(10):738–746
12. Freinkel RK (2001) The biology of the skin. Parthenon Publishing Group, New York
13. Mendonca RJ (2012) Angiogenesis in wound healing. Tissue regeneration—from basic biology to clinical application
14. Eming SA et al (2007) Regulation of angiogenesis: wound healing as a model. Prog Histochem Cytochem 42(3):115–170
15. DiPietro LA (2013) Angiogenesis and scar formation in healing wounds. Curr Opin Rheumatol 25(1):87–91
16. Gronniger E et al (2010) Aging and chronic sun exposure cause distinct epigenetic changes in human skin. PLoS Genet 6(5):e1000971
17. Schmittgen TD, Livak KJ (2008) Analyzing real-time PCR data by the comparative C(T) method. Nat Protoc 3(6):1101–1108
18. Bronneke S et al (2012) DNA methylation regulates lineage-specifying genes in primary lymphatic and blood endothelial cells. Angiogenesis 15(2):317–329
19. Kiistala U (1968) Suction blister device for separation of viable epidermis from dermis. J Invest Dermatol 50(2):129–137
20. Kool J et al (2007) Suction blister fluid as potential body fluid for biomarker proteins. Proteomics 7(20):3638–3650
21. Kanitakis J (2002) Anatomy, histology and immunohistochemistry of normal human skin. Eur J Dermatol 12(4):390–399; quiz 400–401
22. Fritsch P (2004) Aufbau und Funktionen der Haut. In: Dermatologie und Venerologie. Springer, Berlin. 2. Auflage
23. Braverman IM (1997) The cutaneous microcirculation: ultrastructure and microanatomical organization. Microcirculation 4(3):329–340
24. Werner S, Grose R (2003) Regulation of wound healing by growth factors and cytokines. Physiol Rev 83(3):835–870
25. Nissen NN et al (1998) Vascular endothelial growth factor mediates angiogenic activity during the proliferative phase of wound healing. Am J Pathol 152(6):1445–1452
26. Brown LF et al (1992) Expression of vascular permeability factor (vascular endothelial growth factor) by epidermal keratinocytes during wound healing. J Exp Med 176(5):1375–1379
27. Liang CC, Park AY, Guan JL (2007) In vitro scratch assay: a convenient and inexpensive method for analysis of cell migration in vitro. Nat Protoc 2(2):329–333
28. Vitorino P, Meyer T (2008) Modular control of endothelial sheet migration. Genes Dev 22(23):3268–3281
29. Brown NJ et al (2002) Angiogenesis induction and regression in human surgical wounds. Wound Repair Regen 10(4):245–251

30. Roy S et al (2007) Transcriptome-wide analysis of blood vessels laser captured from human skin and chronic wound-edge tissue. Proc Natl Acad Sci USA 104(36):14472–14477
31. Cooper L et al (2005) Wound healing and inflammation genes revealed by array analysis of 'macrophageless' PU.1 null mice. Genome Biol 6(1):R5
32. Chen L et al (2010) *Positional differences in the wound transcriptome of skin and oral mucosa.* BMC Genomics 11:471
33. Roy S et al (2008) Characterization of the acute temporal changes in excisional murine cutaneous wound inflammation by screening of the wound-edge transcriptome. Physiol Genomics 34(2):162–184
34. Sullivan TP et al (2001) The pig as a model for human wound healing. Wound Repair Regen 9(2):66–76
35. Rodero MP, Khosrotehrani K (2010) Skin wound healing modulation by macrophages. Int J Clin Exp Pathol 3(7):643–653
36. Morris MR et al (2010) Genome-wide methylation analysis identifies epigenetically inactivated candidate tumour suppressor genes in renal cell carcinoma. Oncogene 30(12):1390–1401
37. Zhou J et al (2005) A novel six-transmembrane protein hhole functions as a suppressor in MAPK signaling pathways. Biochem Biophys Res Commun 333(2):344–352
38. Barrientos T et al (2007) Two novel members of the ABLIM protein family, ABLIM-2 and -3, associate with STARS and directly bind F-actin. J Biol Chem 282(11):8393–8403
39. Carmeliet P, Tessier-Lavigne M (2005) Common mechanisms of nerve and blood vessel wiring. Nature 436(7048):193–200
40. Presta M et al (2005) Fibroblast growth factor/fibroblast growth factor receptor system in angiogenesis. Cytokine Growth Factor Rev 16(2):159–178
41. Boilly B et al (2000) FGF signals for cell proliferation and migration through different pathways. Cytokine Growth Factor Rev 11(4):295–302
42. Peterson SM et al (2010) Human Sulfatase 2 inhibits in vivo tumor growth of MDA-MB-231 human breast cancer xenografts. BMC Cancer 10:427
43. Baluk P, Hashizume H, McDonald DM (2005) Cellular abnormalities of blood vessels as targets in cancer. Curr Opin Genet Dev 15(1):102–111
44. Ozawa MG et al (2008) Beyond receptor expression levels: the relevance of target accessibility in ligand-directed pharmacodelivery systems. Trends Cardiovasc Med 18(4):126–132
45. Ai X et al (2007) SULF1 and SULF2 regulate heparan sulfate-mediated GDNF signaling for esophageal innervation. Development 134(18):3327–3338